Beam Loss in the Superconducting Quadrupoles of Extraction Line for 14 mrad Crossing Angle

A.I.Drozhdin, N.V.Mokhov, S.I.Striganov, X.Yang

Fermi National Accelerator Laboratory

P.O. Box 500, Batavia, Illinois 60510

June 20, 2008

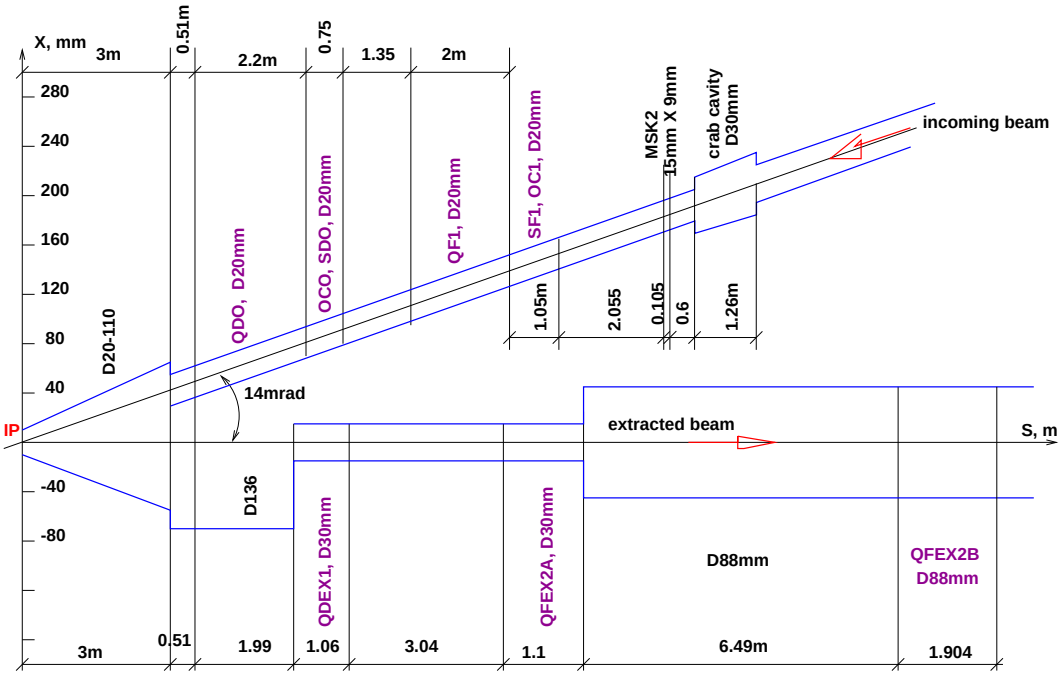

Figure 1: Beam pipe aperture of final doublet and extraction line upstream and downstream of IP.

parameter	ILC-500 nominal	ILC-1000 nominal	ILC-1000 high lumin.
Center of mass energy, GeV	500	1000	1000
Geometric luminosity, $m^{-2}s^{-1}$	1.20e+38	1.85e+38	4.54e+38
Luminosity, $m^{-2}s^{-1}$	2.03e+38	2.82e+38	7.88e+38
Number of particles per bunch	2.0e+10	2.0e+10	2.0e+10
Number of bunches per train	2820	2820	2820
Separation between bunches, ns	307.7	307.7	307.7
Repetition frequency, Hz	5	4	4
Average current (each beam), μa	45.1	36.1	36.1
Beam power (each beam), MW	11.3	18.1	18.1
Relative energy spread (σ)	0.0014	0.001	
Longitudinal beamsize (σ), μm	300.0	300.0	
Horiz. normalized emittance (σ), mm·mrad	10	10	
Vert. normalized emittance (σ), mm·mrad	0.03	0.04	
Horizontal emittance (σ), mm·mrad	2.044E-05	1.022e-05	
Vertical emittance (σ), mm·mrad	6.132E-08	4.088e-08	
Horizontal beta function in IP, mm	15.233	30	
Vertical beta function in IP, mm	0.408	0.3	
Horizontal beam size in IP (σ), nm	553	554	
Vertical beam size in IP (σ), nm	6	3.5	
Horiz. normalized emittance (σ), mm·mrad	30.57	31.25	
Vert. normalized emittance (σ), mm·mrad	0.09622	0.08859	
Disrupted Horizontal emittance (σ), mm·mrad	6.249E-05	3.194E-05	
Disrupted Vertical emittance (σ), mm·mrad	1.967E-07	9.054E-08	
Disrupted Horizontal beta function in IP, mm	6.835	9.673	
Disrupted Horizontal alpha in IP	1.857	1.840	
Disrupted Vertical beta function in IP, mm	0.3633	0.3401	
Disrupted Vertical alpha in IP	0.6983	0.6153	
Disrupted Horizontal beam size in IP (σ), nm	653.6	555.8	
Disrupted Horizontal divergence in IP (σ), mrad	0.2016	0.1203	
Disrupted Vertical beam size in IP (σ), nm	8.453	5.549	
Disrupted Vertical divergence in IP (σ), mrad	2.838E-02	1.916E-02	

Table 1: ILC beam parameters used in calculations.

CM energy	Δy offset [nm]	Total electron loss (kW)				Total BS photon loss (kW)				Total SR photon loss (kW)			
		prior to collim.	Collimators 1	2	3	prior to collim.	Collimators 1	2	3	prior to collim.	Collimators 1	2	3
0.5 TeV	0	2.02	39.0	230	45.6	0	1.8	28.1	0	4.48	2.23	1.48	0.20
high-L (c15)	120	22.7	477	582	52.5	0.51	135.5	193.5	0	4.24	2.4	1.54	0.204
1.0 TeV	0	0.24	0.46	0.39	0.0	0.0	0.0	0.0	0.0	56.9	27.2	18.9	3.0
nominal (c21)	100	2.29	1.20	13.6	2.5	0.0	0.0	0.12	0.0	54.9	25.4	17.9	3.0
1.0 TeV	0	104	31.5	378	60.0	0.013	1.21	7.15	0.0	50.02	22.3	14.9	2.16
high-L (c25)	80	261	585	1404	67.8	0.97	45.45	273	0	45.6	20.9	14.1	1.91

Table 2: Disrupted beam power loss in the extraction line for 0.75 mrad photon aperture model. All elements of beam line downstream of IP, including collimators, have round or elliptical aperture. Electron loss prior collimators are calculated using tail 1 and 2, losses in the collimators are calculated using beam 1 and 2.

CM energy	Δy offset [nm]	Total electron loss (kW)				Total BS photon loss (kW)				Total SR photon loss (kW)			
		prior to collim.	Collimators 1	2	3	prior to collim.	Collimators 1	2	3	prior to collim.	Collimators 1	2	3
0.5 TeV	0	1.31	40.2	230	45.6	0	1.8	28.05	0	1.82	4.89	1.47	0.204
high-L (c15)	120	6.01	492	585	52.2	0	136.05	193.5	0	1.82	4.80	1.54	0.21
1.0 TeV	0	0.12	0.62	0.39	0.0	0.0	0.0	0.0	0.0	23.5	60.6	18.9	3.0
nominal (c21)	100	1.32	1.67	13.4	2.34	0.0	0.0	0.12	0.0	22.9	57.6	18.1	2.7
1.0 TeV	0	79.3	54.6	375	60.3	0.0	1.23	7.17	0.0	20.9	51.6	14.9	2.16
high-L (c25)	80	216	630	1404	64.2	0.0035	46.5	273	0.0	20.5	46.2	14.1	1.92

Table 3: Disrupted beam power loss in the extraction line for 1.25 mrad photon aperture model. All elements of beam line downstream of IP, including collimators, have round or elliptical aperture. Electron loss prior collimators are calculated using tail 1 and 2, losses in the collimators are calculated using beam 1 and 2.

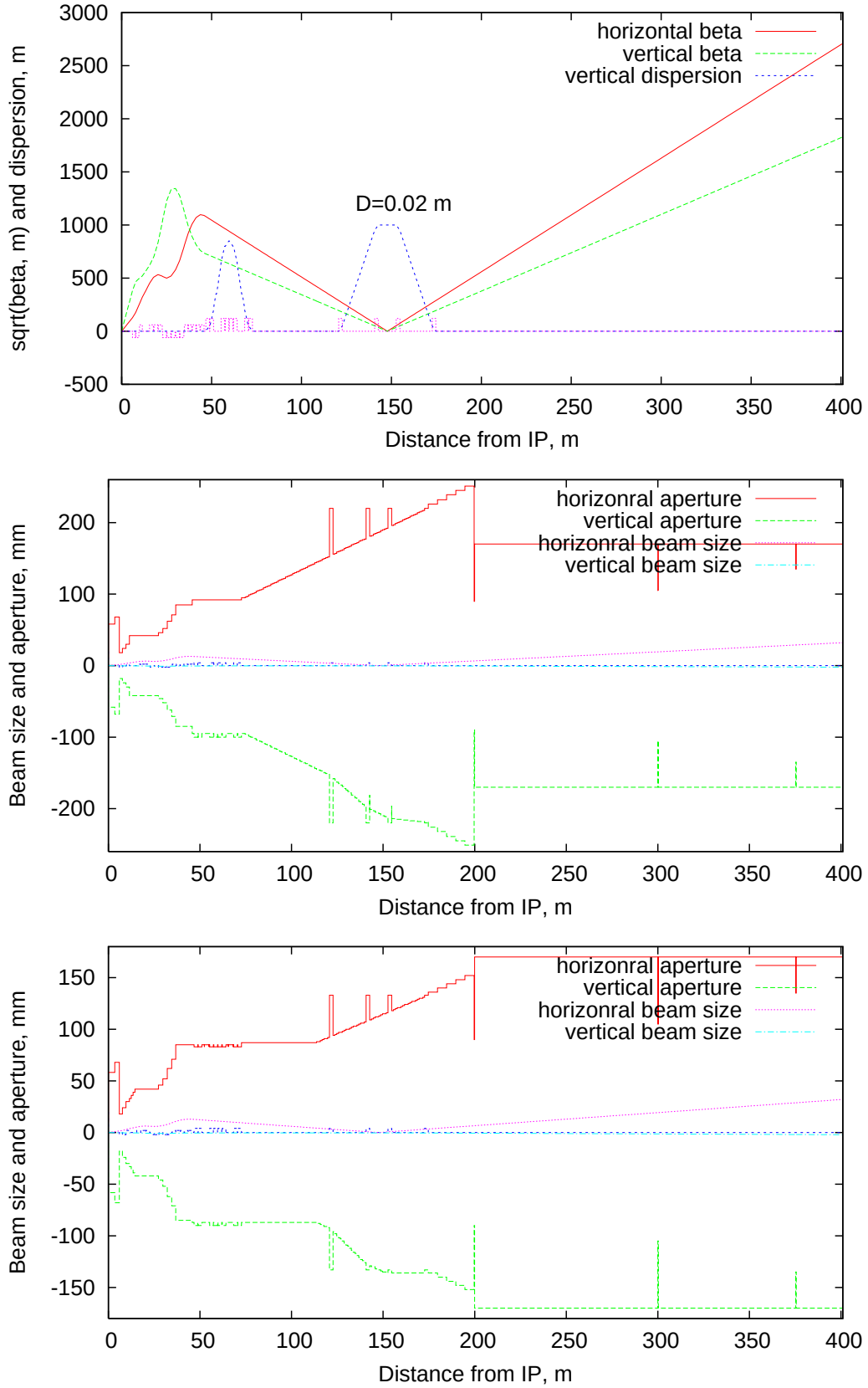

Figure 2: SQRT($\beta_{x,y}$) and vertical dispersion (top) in the extraction beam line for 1000 GeV CM, and aperture for photon angle 1.25 mrad (middle) and 0.75 mrad (bottom).

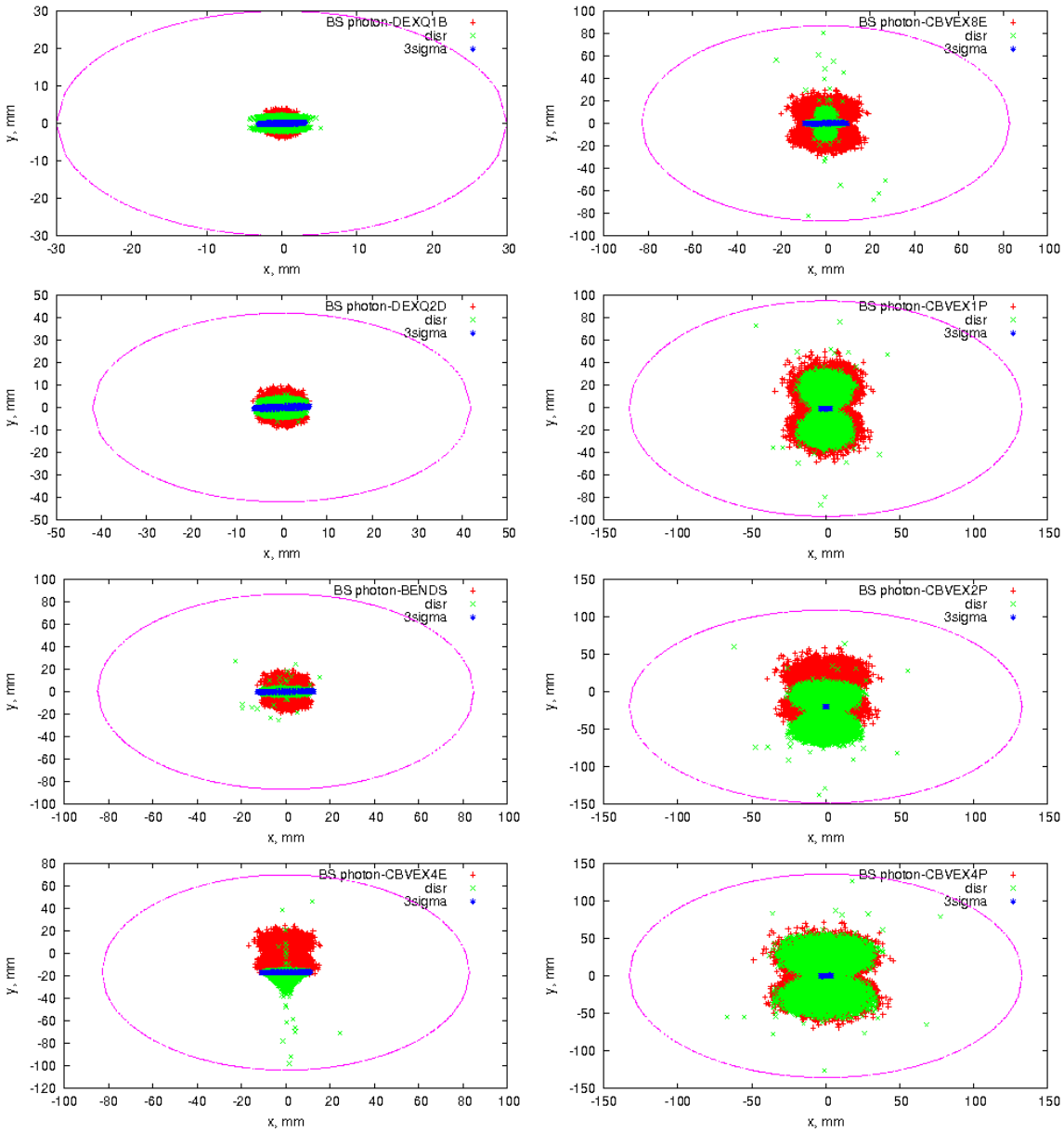

Figure 3: In the case of 0.75 mrad photon aperture, disrupted beam (file *beam*1*and*2 from *cs*21_*dy*100_*hs*) with vertical offset at IP of 100 nm (green), 3 sigma beam (blue) and beamstrahlung photon (file *photon.dat* from *cs*21_*dy*100_*hs*) beam (red) are printed out at DEXQ1B, DEXQ2D, BENDS, CBVEX4E, CBVEX8E, CBVEX1P, CBVEX2P, and CBVEX4P in the order of top to bottom and left to right.

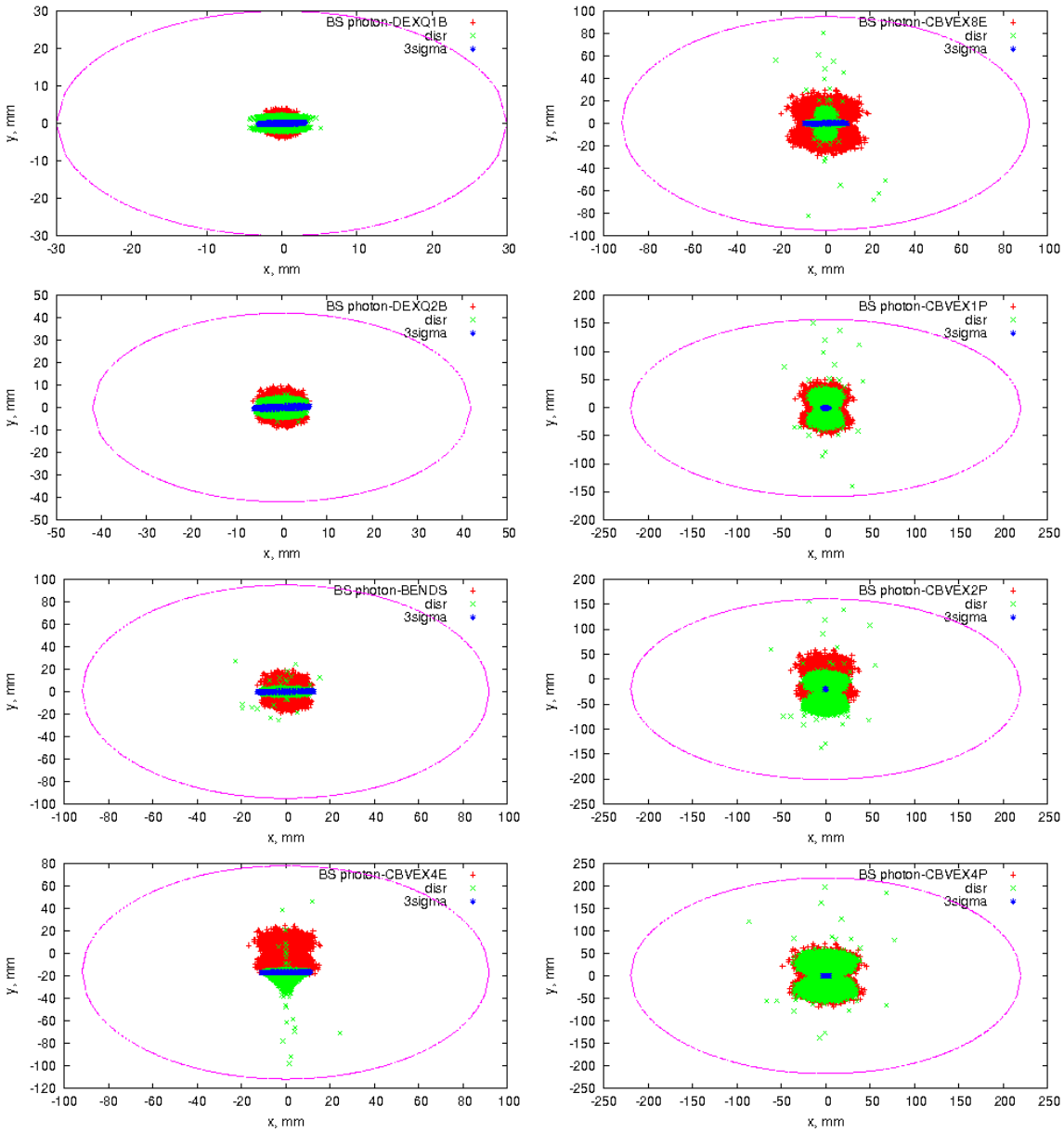

Figure 4: In the case of 1.25 mrad photon aperture, disrupted beam (file *beam*1*and*2 from *cs*21_*dy*100_*hs*) with vertical offset at IP of 100 nm (green), 3 sigma beam (blue) and beamstrahlung photon (file *photon.dat* from *cs*21_*dy*100_*hs*) beam (red) are printed out at DEXQ1B, DEXQ2D, BENDS, CBVEX4E, CBVEX8E, CBVEX1P, CBVEX2P, and CBVEX4P in the order of top to bottom and left to right.

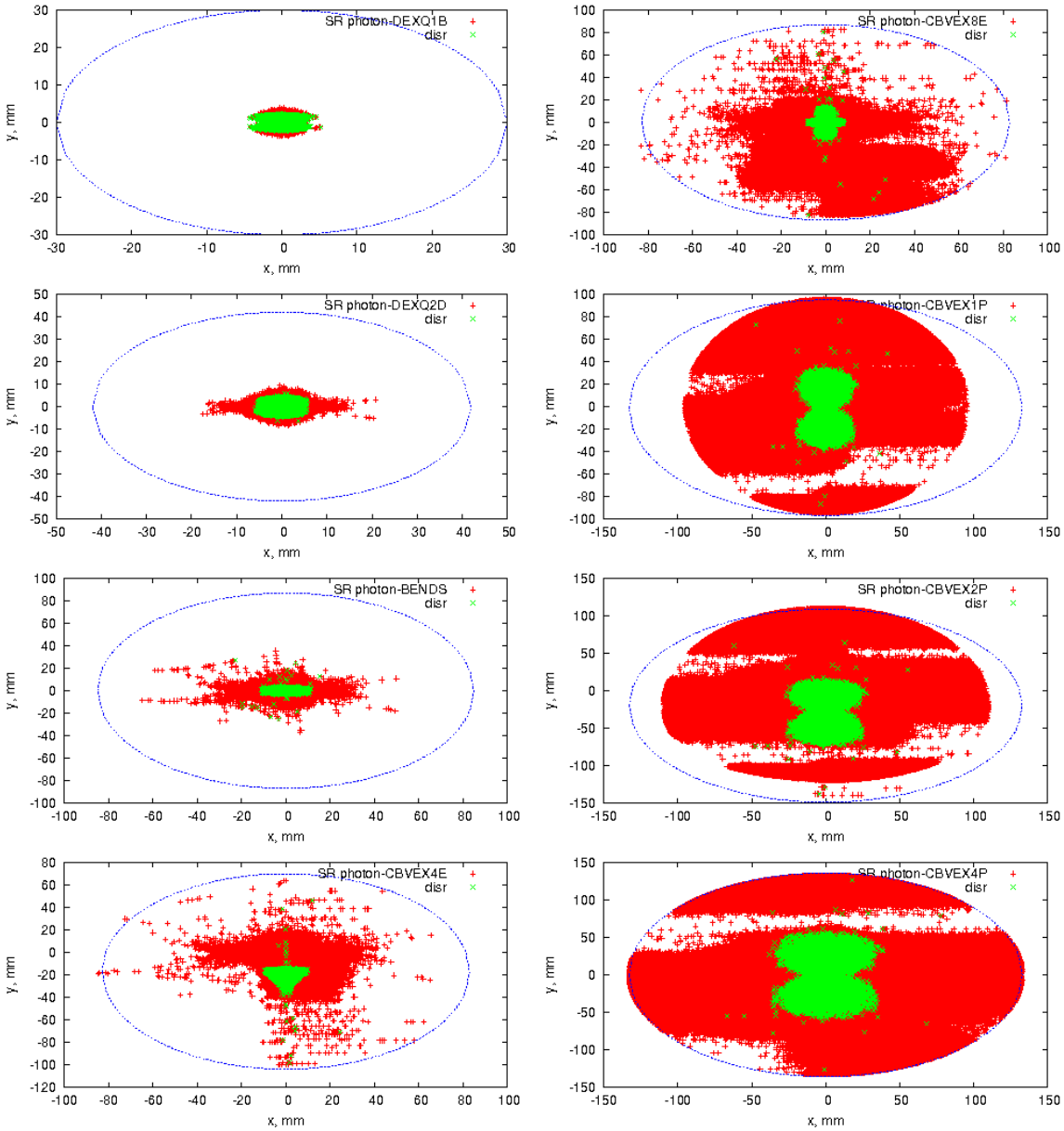

Figure 5: In the case of 0.75 mrad photon aperture, disrupted beam (file *beam*1*and*2 from *cs*21_*dy*100_*hs*) with vertical offset at IP of 100 nm (green) and synchrotron radiated photons (red) from the disrupted beam are printed out at DEXQ1B, DEXQ2D, BENDS, CBVEX4E, CBVEX8E, CBVEX1P, CBVEX2P, and CBVEX4P in the order of top to bottom and left to right.

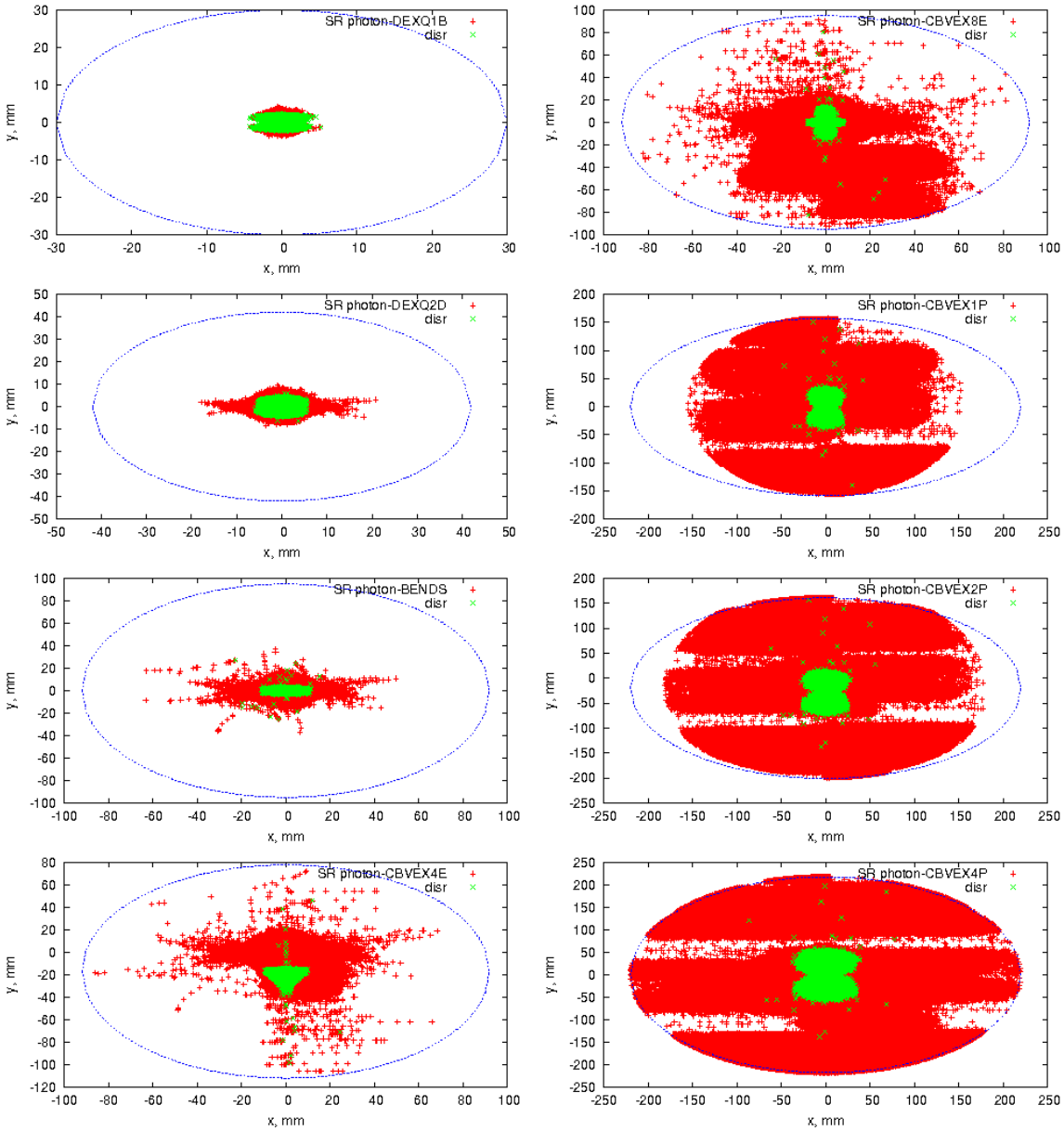

Figure 6: In the case of 1.25 mrad photon aperture, disrupted beam (file *beam*1*and*2 from *cs*21_*dy*100_*hs*) with vertical offset at IP of 100 nm (green) and synchrotron radiated photons (red) from the disrupted beam are printed out at DEXQ1B, DEXQ2D, BENDS, CBVEX4E, CBVEX8E, CBVEX1P, CBVEX2P, and CBVEX4P in the order of top to bottom and left to right.

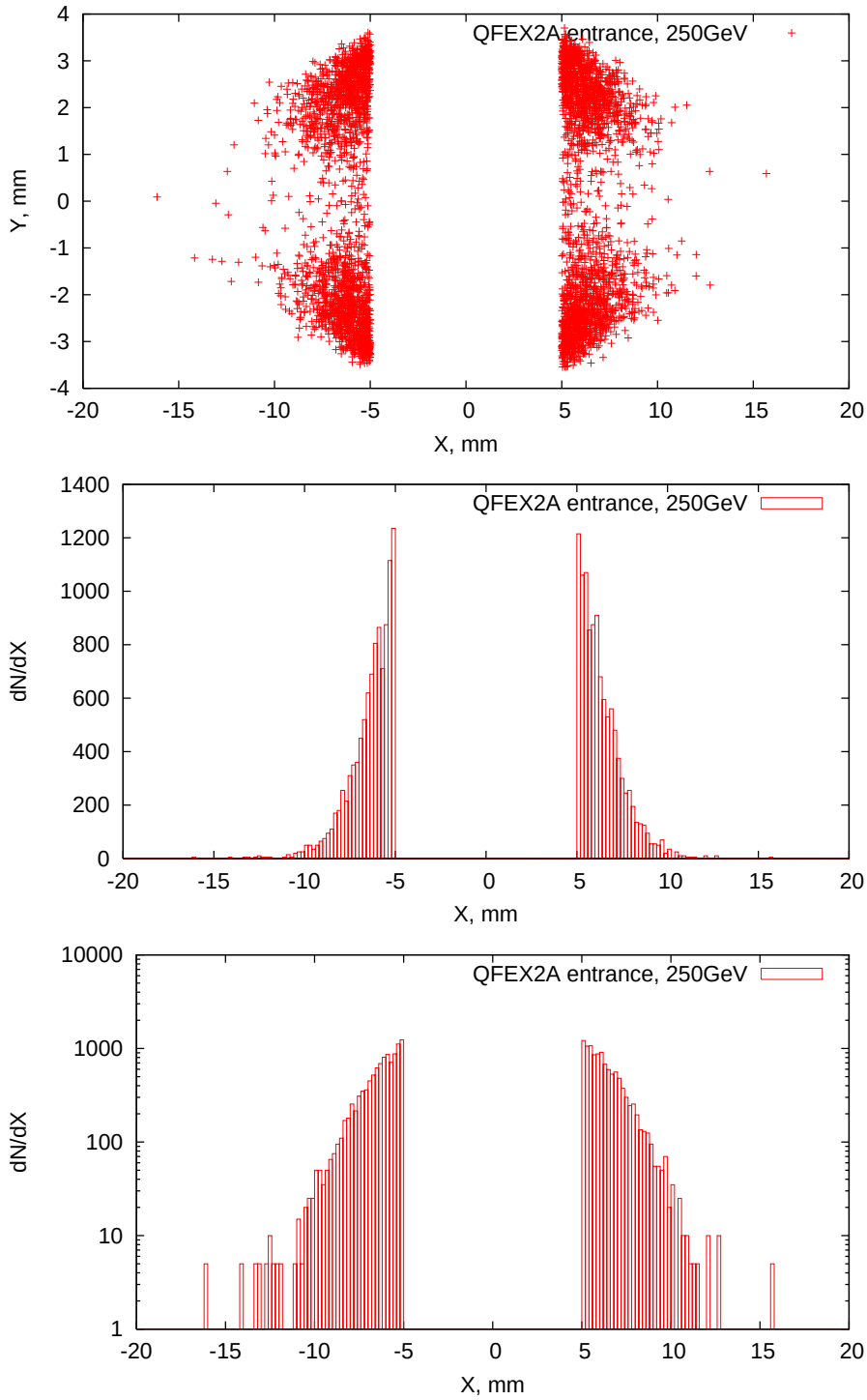

Figure 7: Disrupted beam halo at the QFEX2A entrance for c14-dx0-dy120-tail12-ip-352k.out 250 GeV beam with vertical offset at IP of dX=120 nm. There is no beam loss at first quad QDEX1. Beam loss between first and second quads at the drift DEXQ1 (3.04m long) is ∼14 W/m, at the second quad QFEX2A (1.1m long) is ∼16 W/m. Aperture of the drift DEXQ1 and quads QDEX1, QFEX2A is D=30mm.

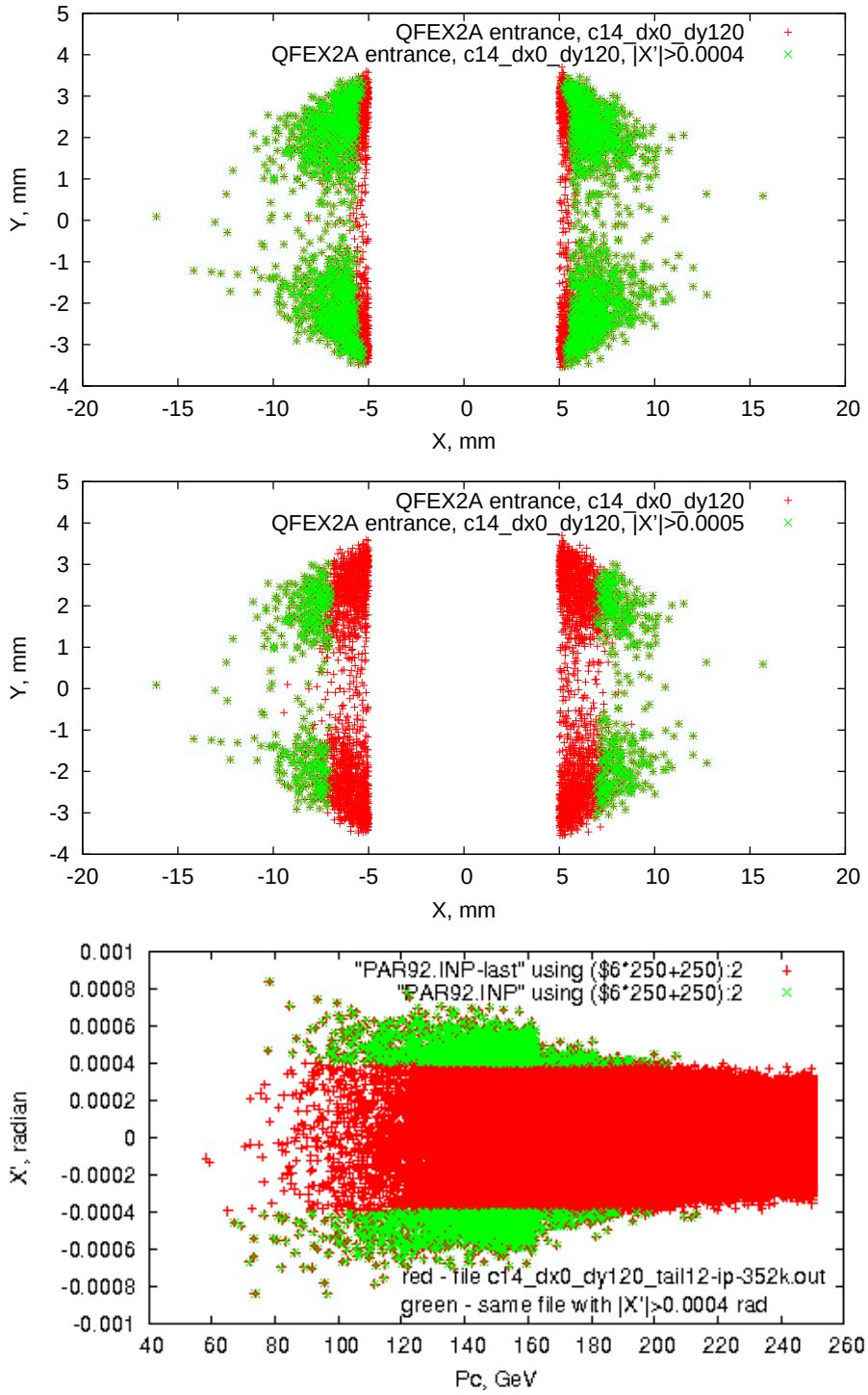

Figure 8: Disrupted beam halo at the QFEX2A entrance for c14-dx0-dy120-tail12-ip-352k.out 250 GeV beam with vertical offset at IP of dX=120 nm (red) and for initial particles from this file with $|X'| > 0.0004$ (top, green). This file consists of 2813 particles instead of 100,000 ones. Only particles with $|X| > 5mm$ are shown here at the QFEX2A entrance. We loose the same 4 particles at the QFEX2A quad in both cases. Initial particle distribution is shown on the bottom. It would be good to increase the number of particle lost at QFEX2A by increasing of initial number of particle in a file with $|X'| > 0.0004$ from 2813 to 281,300. Increasing X' to $|X'| > 0.0005$ in the initial file, it is possible to reduce number of initial particles to 810, having the same 4 particles loss at the QFEX2A quad (middle). So, for increasing statistics of loss at the second quad it would be good to produce initial particle file with $|X'| > 0.0005$. If number of particles at this file is 100,000, we expect to loose about 400-500 particles. It is fine. If this requires too long calculations, statistics can be decreased by a factor of 2-5.

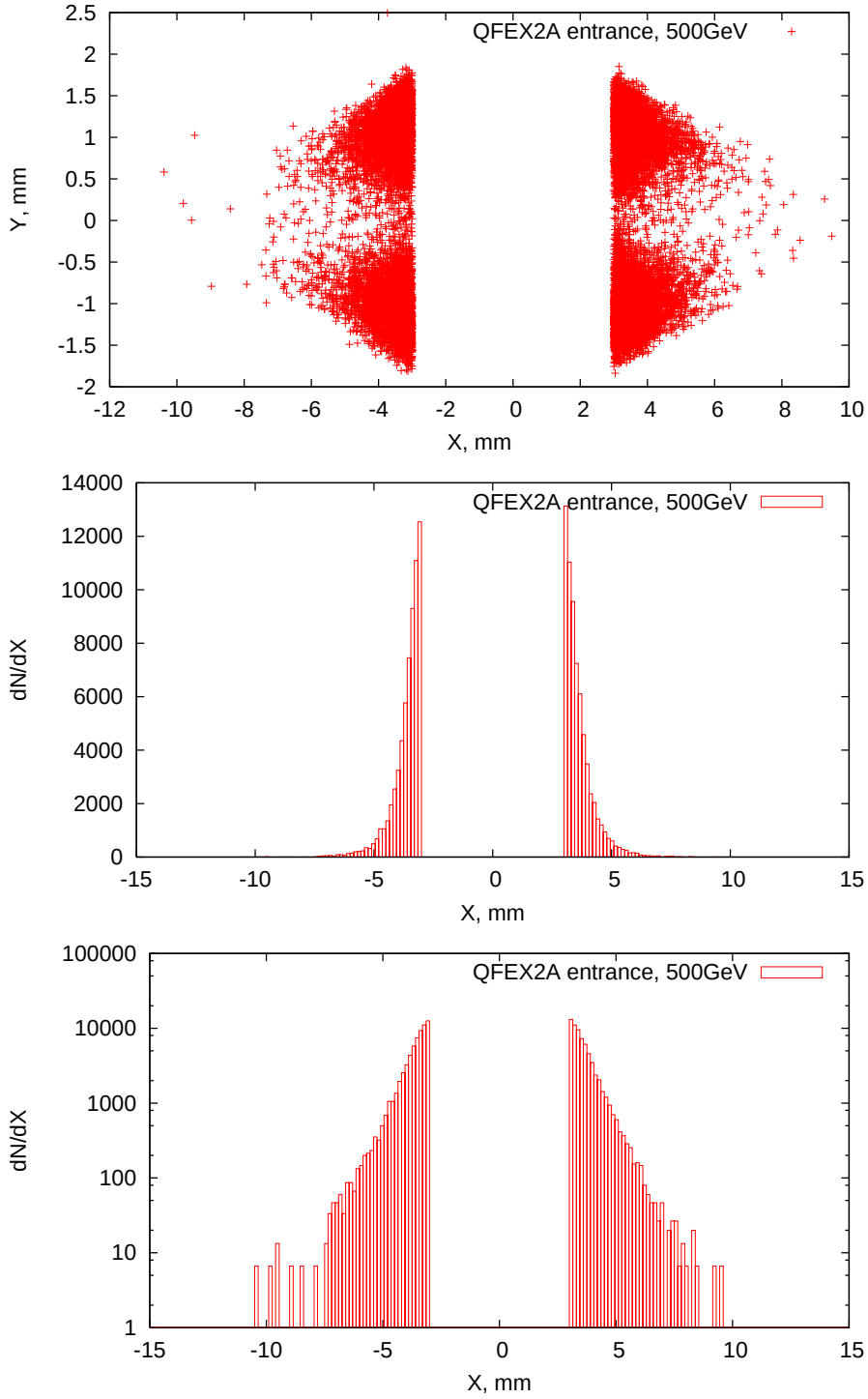

Figure 9: Disrupted beam halo at the QFEX2A entrance for c27-high-L-dx0-dy100-tail12-ip-2.02m.out 500 GeV beam with vertical offset at IP of dX=100 nm. There is no beam loss at first and second quads (QDEX1, QFEX2A). Aperture of the drift DEXQ1 and quads QDEX1, QFEX2A is D=30mm.

S	LOSS	I	lost	APERTURE		LENGTH	NAME
(m)	(W/m)	(GeV/Po)	hor.	ver.	(m)		
6.030	0.000E+00	11	0.0000	15.00	15.00	0.5300	QDEX1S
6.560	0.000E+00	11	0.0000	15.00	15.00	0.5300	QDEX1S
9.500	0.145E+01	13	28.0168	15.00	15.00	2.9400	DEXQ1
9.600	0.128E+02	14	8.4298	15.00	15.00	0.1000	DEXQ2A1
10.150	0.142E+02	15	51.4028	15.00	15.00	0.5500	QFEX2AS
10.700	0.177E+02	16	63.8736	15.00	15.00	0.5500	QFEX2AS

Table 4: Disrupted beam loss distribution at the beginning of 14 mrad extraction line for tail1-2-lt-0-65E0-or-gt-500urad 250 GeV beam (from http://www.slac.stanford.edu/∼seryi/ILC_new_gp_files/2008_cs14_hs/.

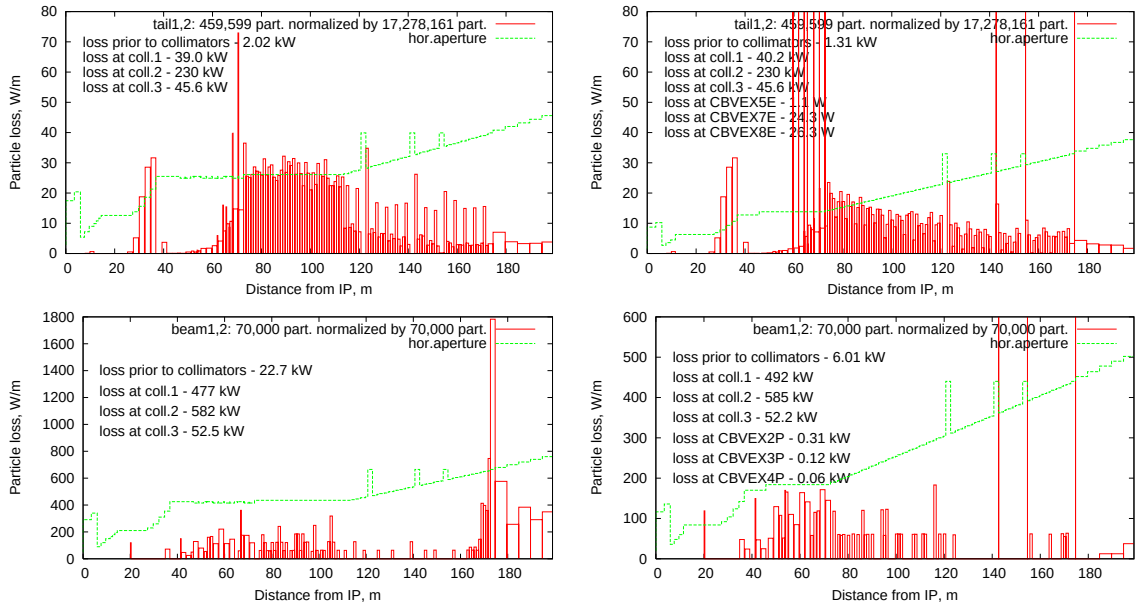

Figure 10: Primary beam loss distribution along the extraction line prior to collimators. Top: for beam without vertical offset at IP (file *tail*1*and*2 from *cs*15_*hs*) for 0.75 mrad (left) and 1.25 mrad (right) photon aperture, and bottom: for beam with vertical offset at IP of 120 nm (file *beam*1*and*2 from *cs*15_*dy*120_*hs*) for 0.75 mrad (left) and 1.25 mrad (right) photon aperture. Beam losses at the collimators are calculated using *beam*1*and*2. All elements of beam line downstream of IP, including collimators, have round or elliptical aperture. The electron and photon loss at the "artificial" collimators located at the entrance and exit to chicane bends shown in Figs. 10 - 15 are not exist in reality. These collimators were included to allow calculation of loss in bends using DIMAD.

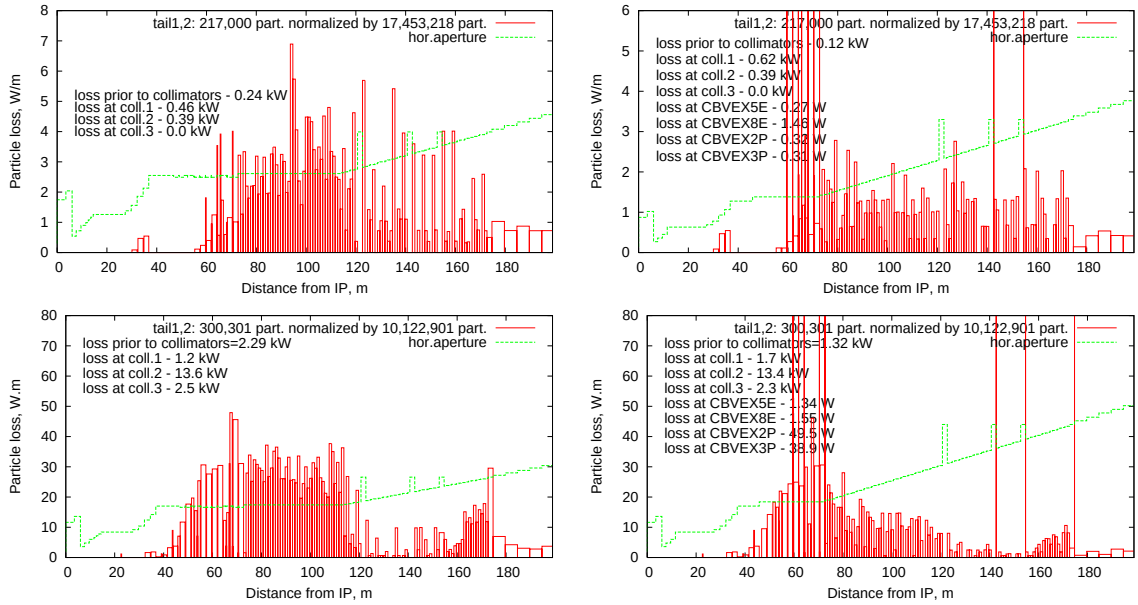

Figure 11: Primary beam loss distribution along the extraction line prior to collimators. Top: for beam without vertical offset at IP (file *tail*1*and*2 from *cs*21_*hs*) for 0.75 mrad (left) and 1.25 mrad (right) photon aperture, and bottom: for beam with vertical offset at IP of 100 nm (file *tail*1*and*2 from *cs*21_*dy*100_*hs*) for 0.75 mrad (left) and 1.25 mrad (right) photon aperture. Beam losses at the collimators are calculated using *beam*1*and*2. All elements of beam line downstream of IP, including collimators, have round or elliptical aperture.

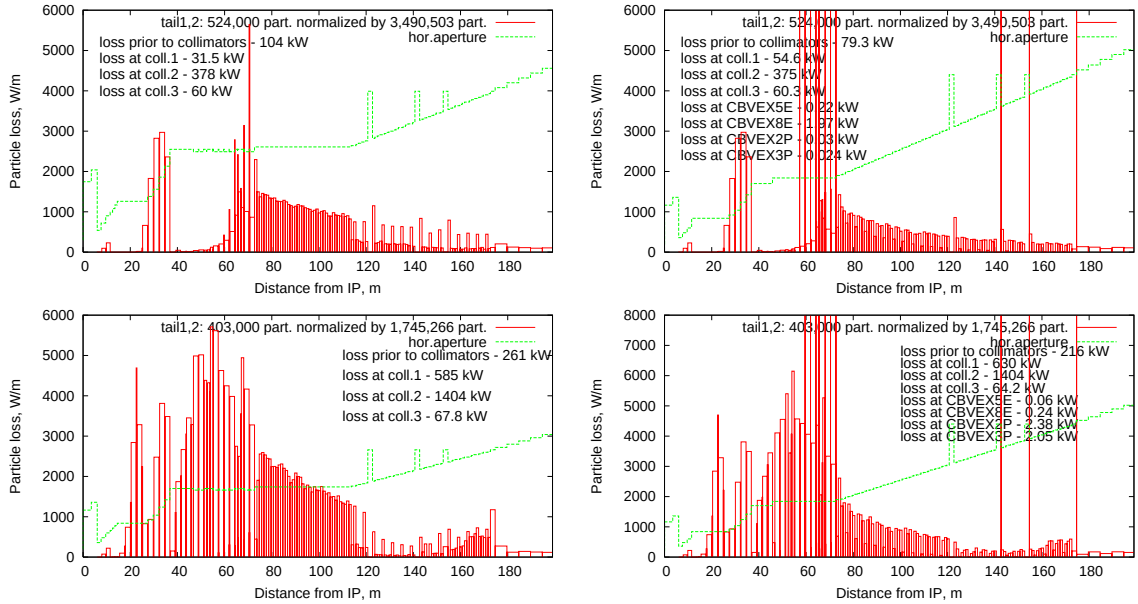

Figure 12: Primary beam loss distribution along the extraction line prior to collimators. Top: for beam without vertical offset at IP (file *tail*1*and*2 from *cs*25_*hs*) for 0.75 mrad (left) and 1.25 mrad (right) photon aperture, and bottom: for beam with vertical offset at IP of 80 nm (file *tail*1*and*2 from *cs*25_*dy*80_*hs*) for 0.75 mrad (left) and 1.25 mrad (right) photon aperture. Beam losses at the collimators are calculated using *beam*1*and*2. All elements of beam line downstream of IP, including collimators, have round or elliptical aperture.

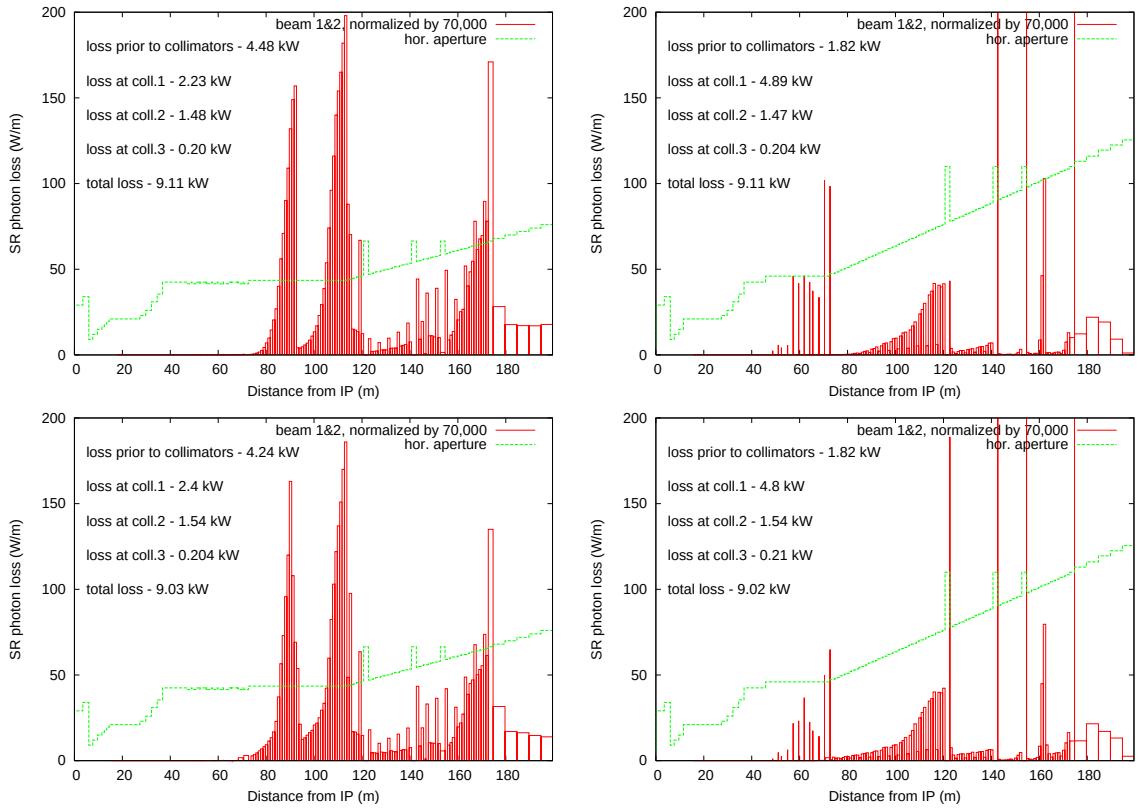

Figure 13: Synchrotron radiation loss distribution along the extraction line prior to collimators. Top: for beam without vertical offset at IP (file *beam*1*and*2 from *cs*15_*hs*) for 0.75 mrad (left) and 1.25 mrad (right) photon aperture, and bottom: for beam with vertical offset at IP of 120 nm (file *beam*1*and*2 from *cs*15_*dy*120_*hs*) for0.75 mrad (left) and 1.25 mrad (right) photon aperture. All elements of beam line downstream of IP, including collimators, have round or elliptical aperture.

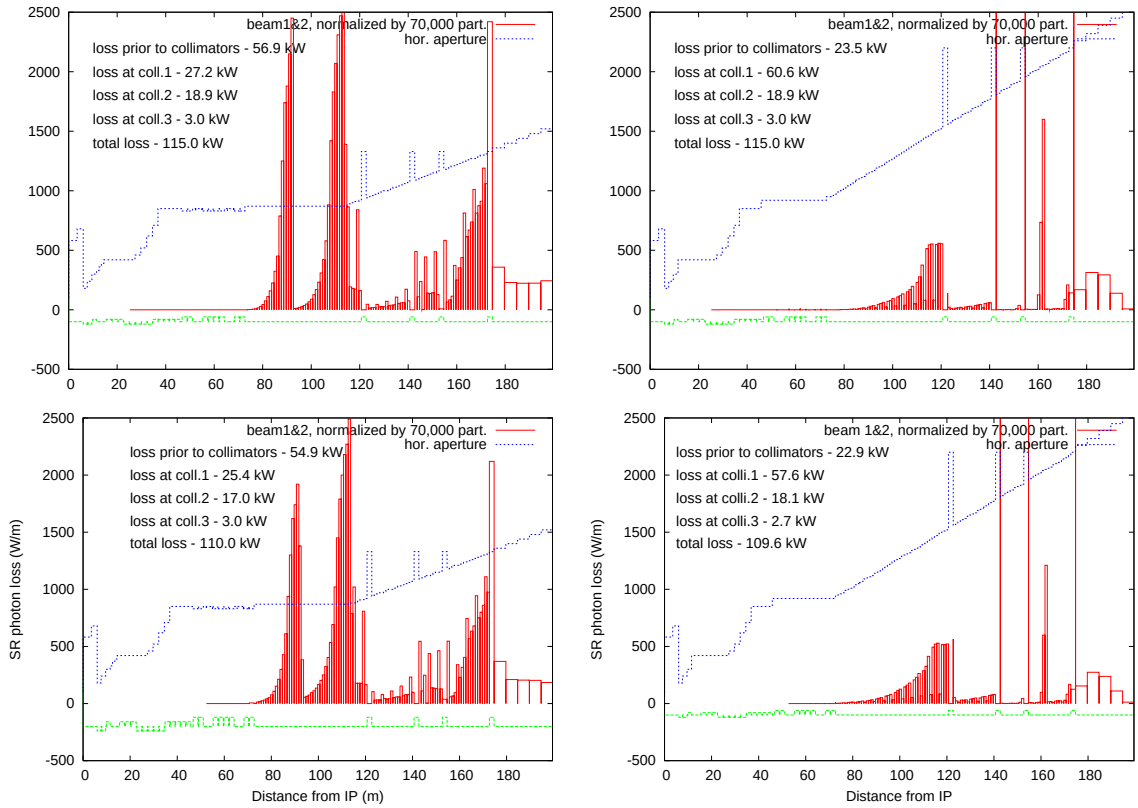

Figure 14: Synchrotron radiation loss distribution along the extraction line prior to collimators. Top: for beam without vertical offset at IP (file *beam*1*and*2 from *cs*21_*hs*) for 0.75 mrad (left) and 1.25 mrad (right) photon aperture, and bottom: for beam with vertical offset at IP of 100 nm (file *beam*1*and*2 from *cs*21_*dy*100_*hs*) for0.75 mrad (left) and 1.25 mrad (right) photon aperture. All elements of beam line downstream of IP, including collimators, have round or elliptical aperture.

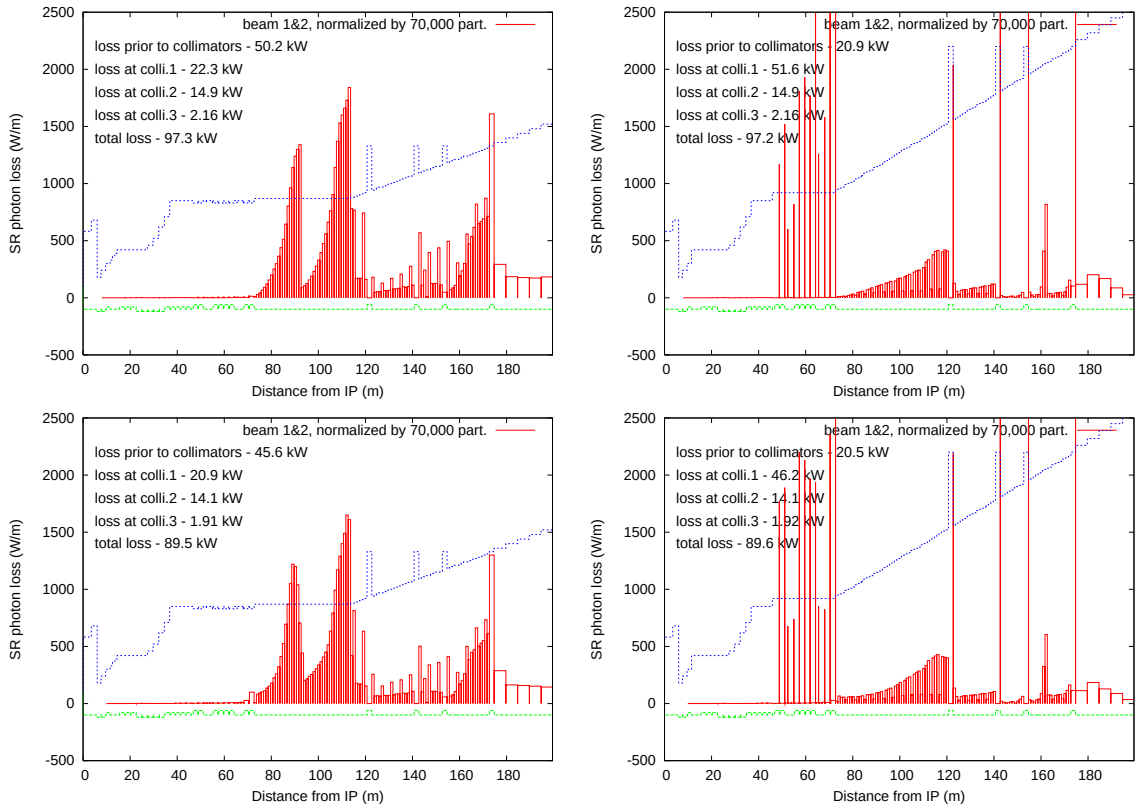

Figure 15: Synchrotron radiation loss distribution along the extraction line prior to collimators. Top: for beam without vertical offset at IP (file *beam*1*and*2 from *cs*25_*hs*) for 0.75 mrad (left) and 1.25 mrad (right) photon aperture, and bottom: for beam with vertical offset at IP of 80 nm (file *beam*1*and*2 from *cs*25_*dy*80_*hs*) for 0.75 mrad (left) and 1.25 mrad (right) photon aperture. All elements of beam line downstream of IP, including collimators, have round or elliptical aperture.

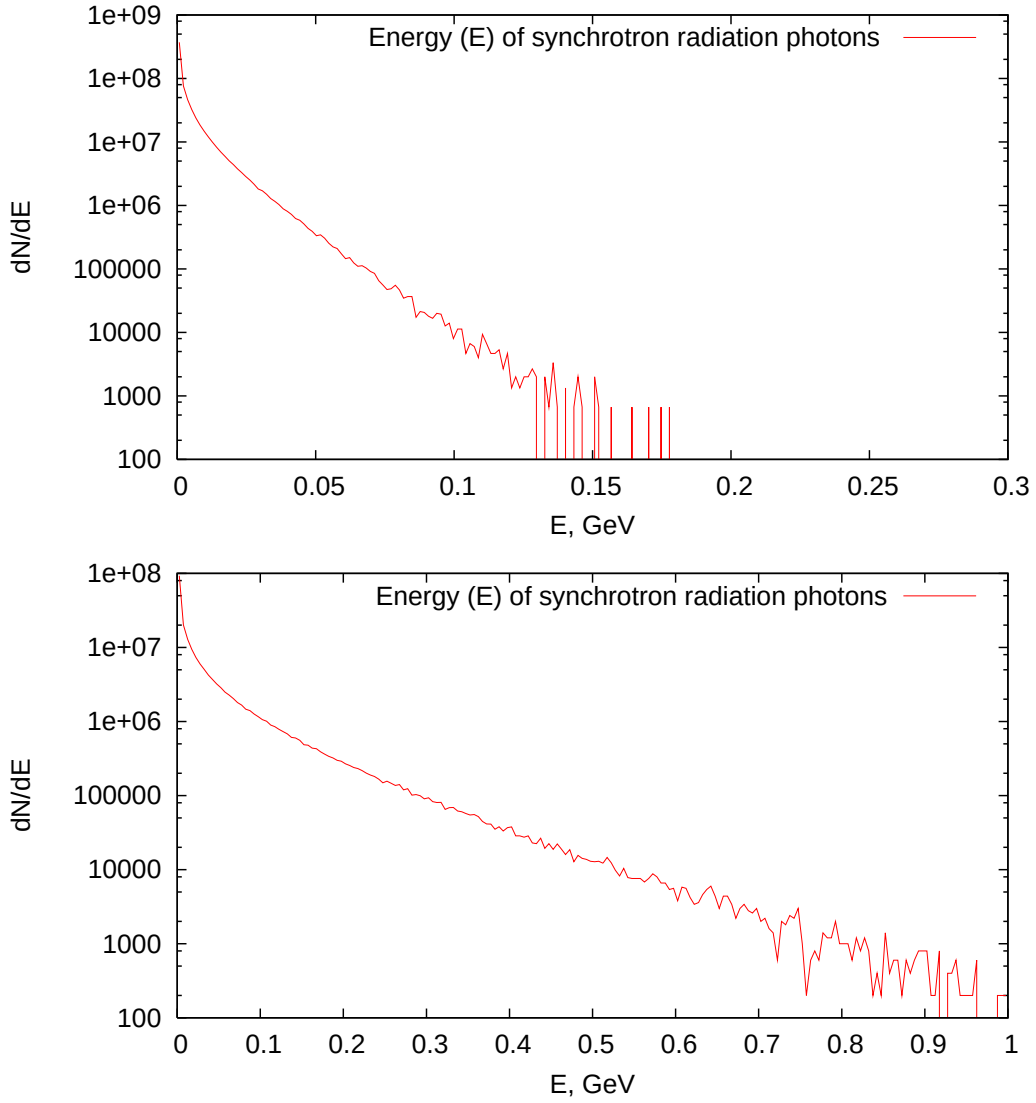

Figure 16: Energy spectrum of synchrotron radiation photons lost in the region of prior to collimators in the extraction line for 0.75 mrad photon aperture in two cases of beam1 and beam2 from *cs*15 (top) and *c*25 (bottom).

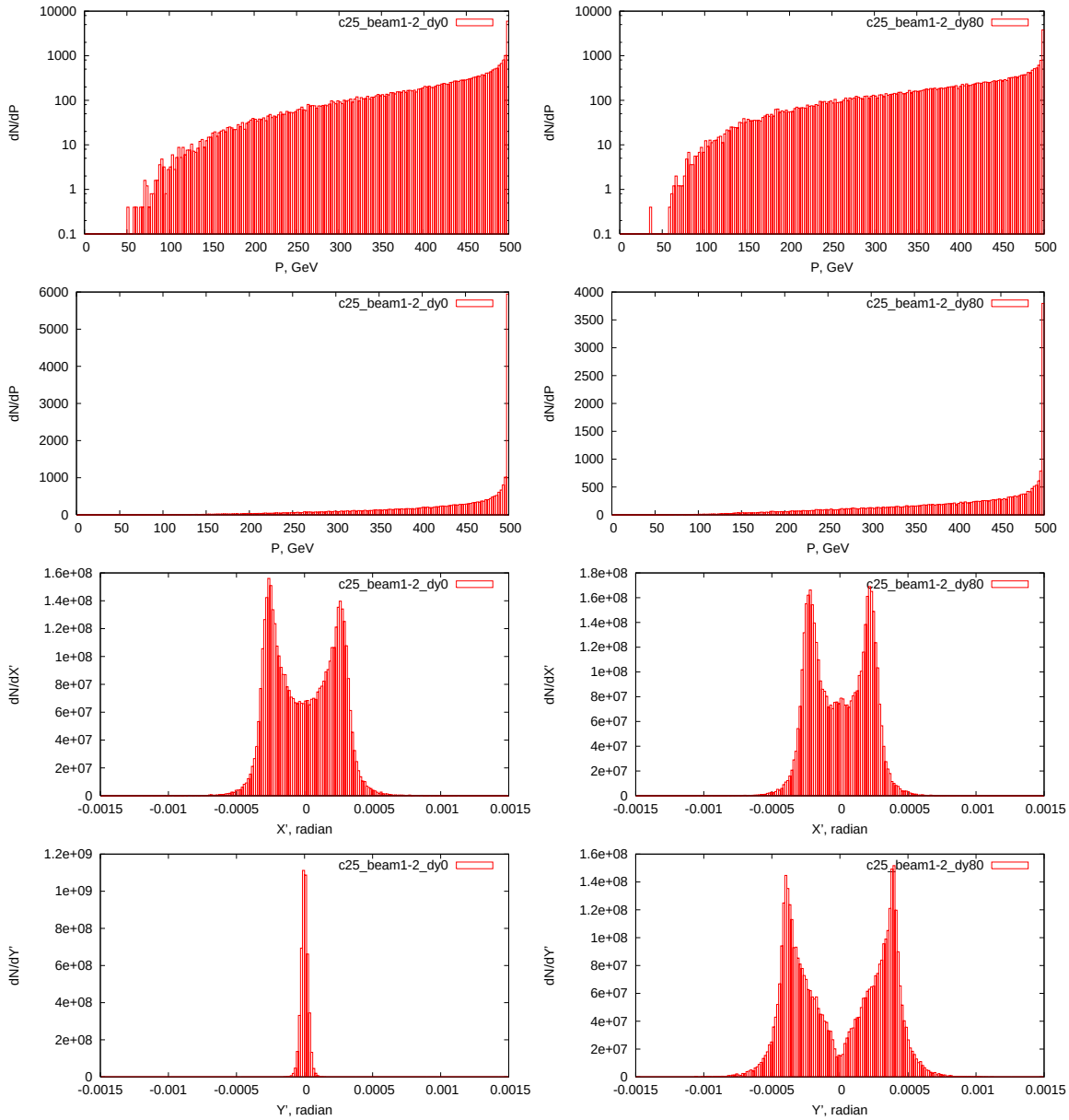

Figure 17: Energy (top) and angular spectrum of initial particles of beam 1 and 2, for files from *c*25*_hs* (left) and *c*25*_dy*80*_hs* (right).

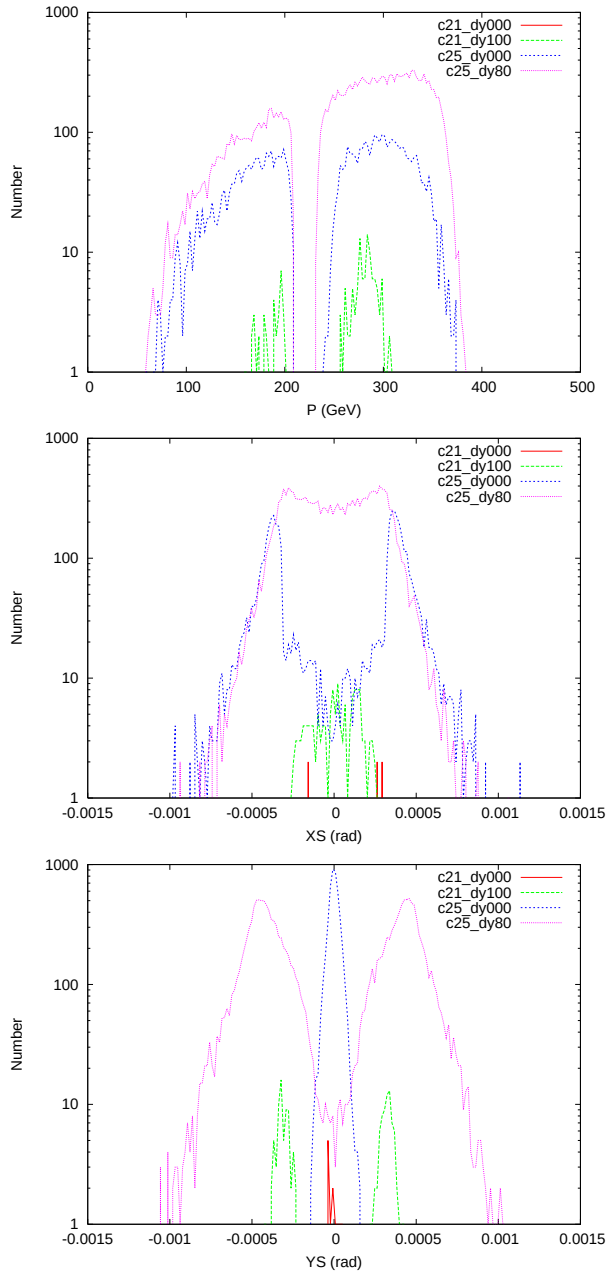

Figure 18: Lost particles' (including loss on final collimators) energy (top) and angular (middle and bottom) spectrum at IP for extraction line with 0.75 mrad photon aperture. Initial particles are: beam 1 and 2, for files from *c*21_*hs*, *c*21_*dy*100_*hs*, *c*25_*hs*, and *c*25_*dy*80_*hs*.

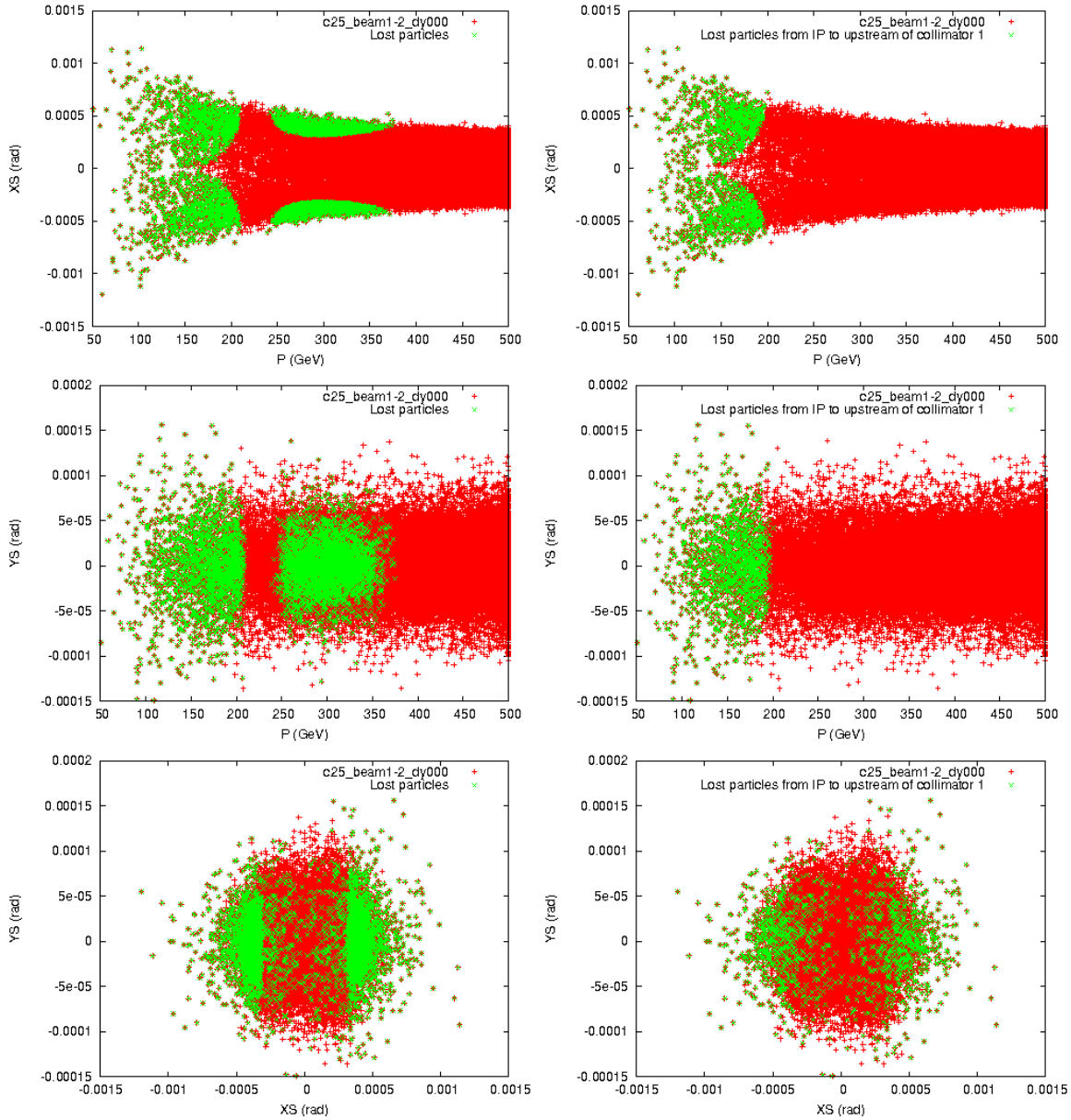

Figure 19: All initial particles of beam 1 and 2 for file *c25_hs* (red). In the left: lost particles in the region from IP to beam dump (green) for extraction line with 0.75 mrad photon aperture, P *vs*. XS (top), P *vs*. YS (middle), and XS *vs*. YS (bottom). In the right: lost particles in the region from IP to upstream of collimator 1 (green), P *vs*. XS (top), P *vs*. YS (middle), and XS *vs*. YS (bottom).

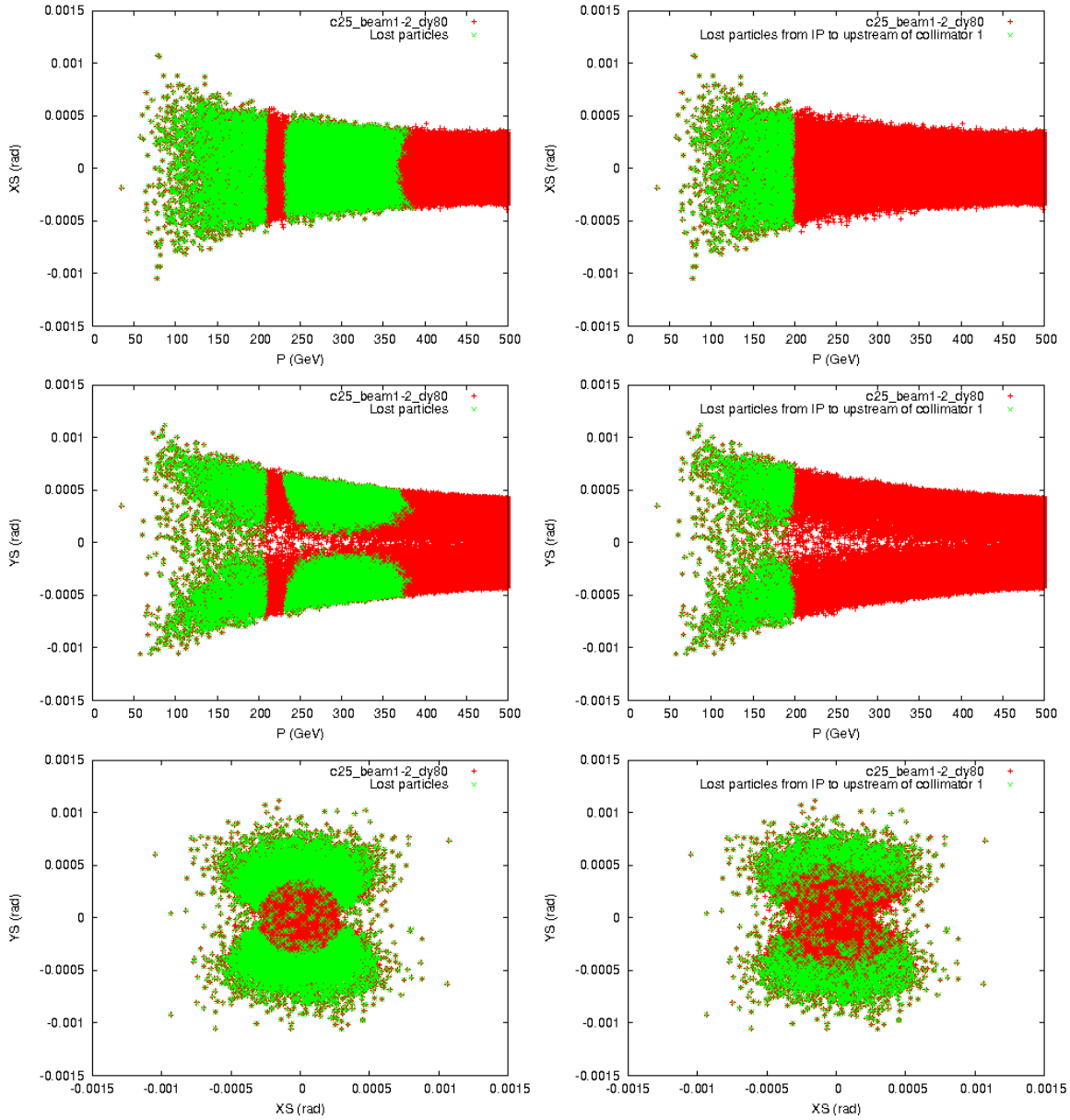

Figure 20: All initial particles of beam 1 and 2 for file *c*25_*dy*80_*hs* (red). In the left: lost particles in the region from IP to beam dump (green) for extraction line with 0.75 mrad photon aperture, P *vs*. XS (top), P *vs*. YS (middle), and XS *vs*. YS (bottom). In the right: lost particles in the region from IP to upstream of collimator 1 (green), P *vs*. XS (top), P *vs*. YS (middle), and XS *vs*. YS (bottom).

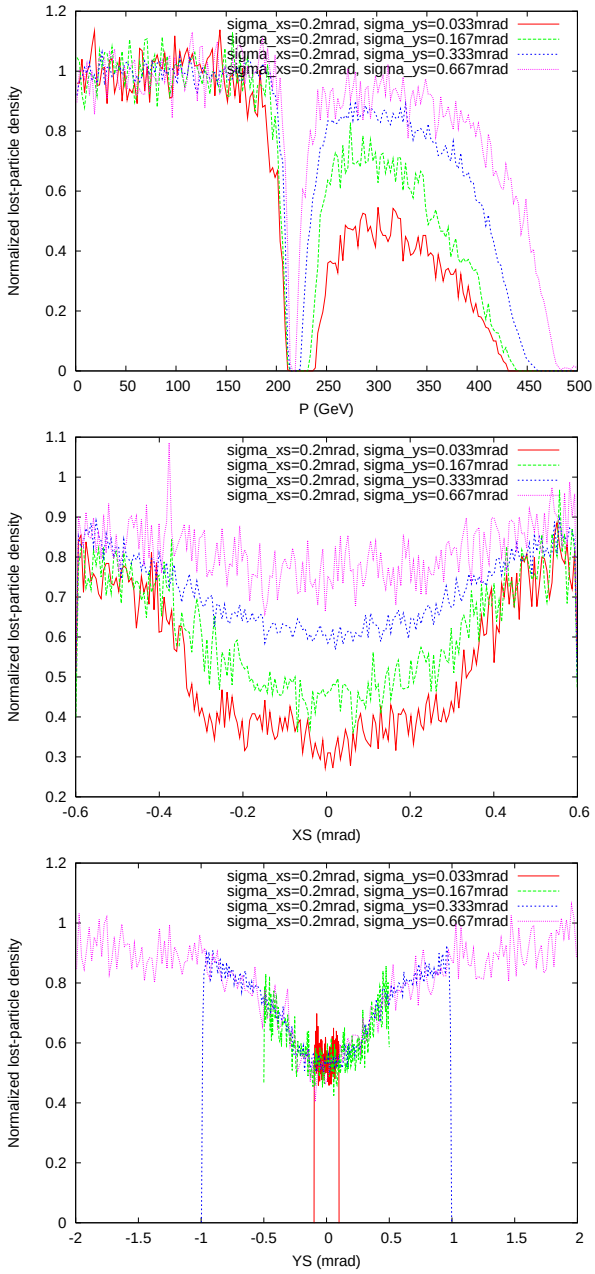

Figure 21: For extraction line with 0.75 mrad photon aperture, initial 100,000 particles at IP are randomly distributed on P (0-500GeV), XS, and YS. σ_{XS} is a constant of 0.2 mrad for all cases, and σ_{YS} is varied among 0.0333 mrad (red), 0.167 mrad (green), 0.333 mrad (blue), and 0.667 mrad (magenta). Histograms of normalized lost-particle density, including loss on final collimators (probability for particle getting lost) in P (top), XS (middle) and YS (bottom).

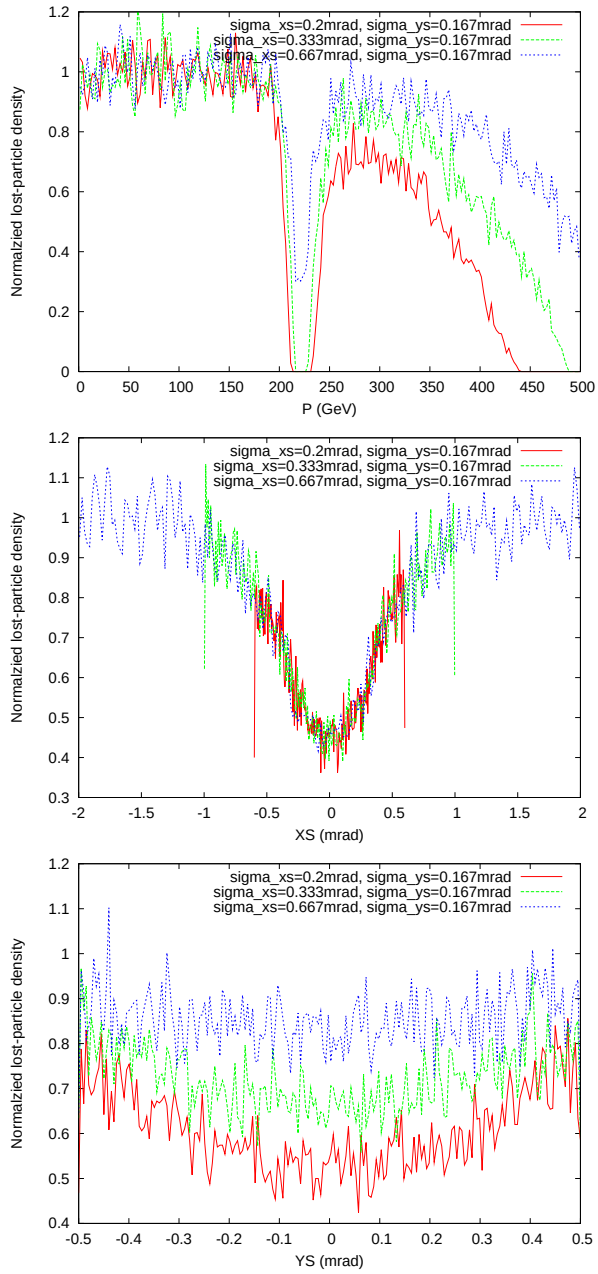

Figure 22: For extraction line with 0.75 mrad photon aperture, initial 100,000 particles are randomly distributed on P (0-500GeV), XS, and YS. σ_{YS} is a constant of 0.167 mrad, and σ_{XS} is varied among 0.2 mrad (red), 0.333 mrad (green), and 0.667 mrad (blue). Histograms of normalized lost-particle density, including loss on final collimators (probability for particle getting lost) in P (top), XS (middle) and YS (bottom).

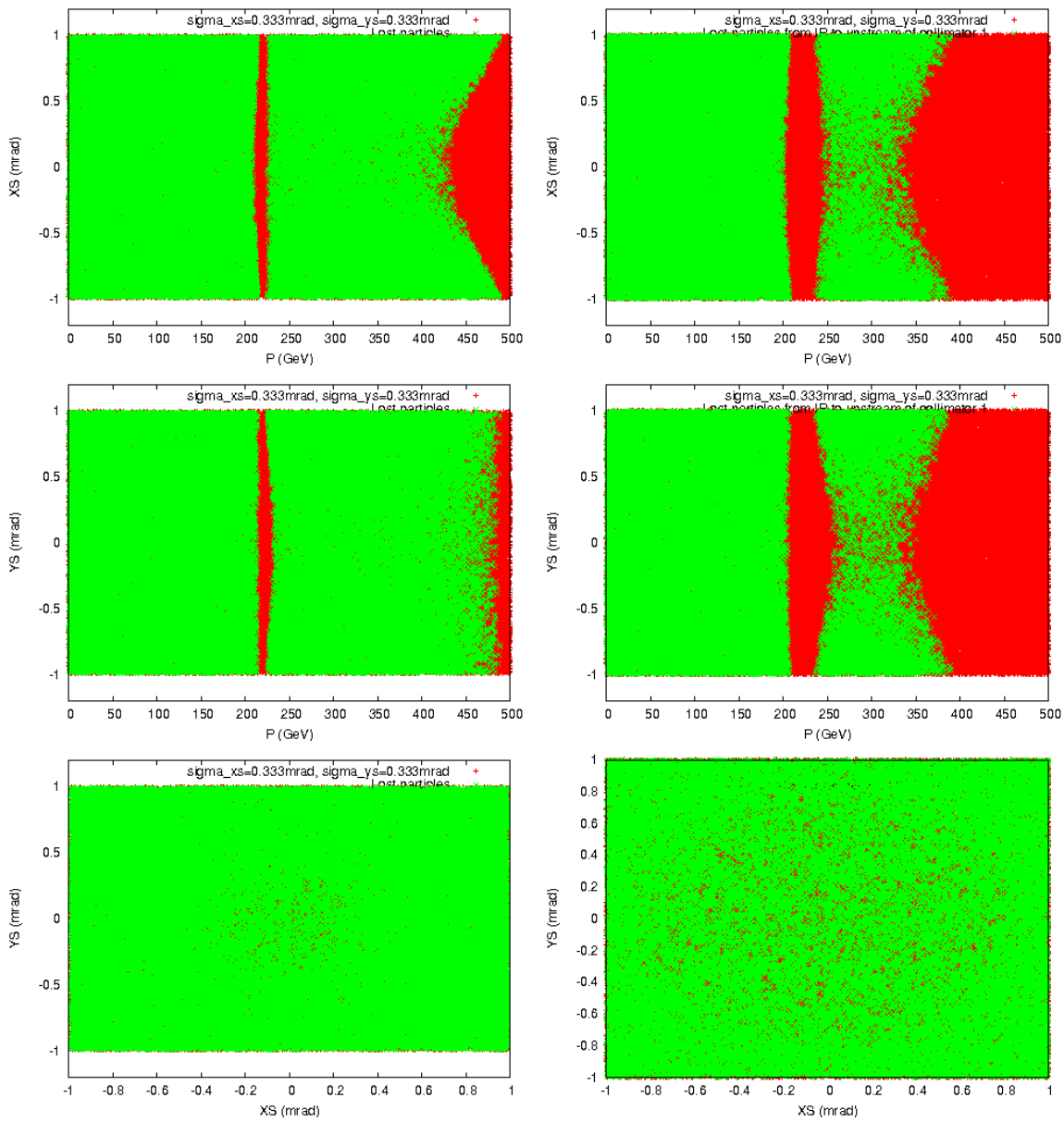

Figure 23: Initial 100,000 particles being randomly distributed in *P* (0-500GeV), *XS* (σ_{xs}=0.333mrad), and *YS* (σ_{ys}=0.333mrad) (red). In the left: lost particles for extraction line with 0.75 mrad photon aperture from IP to beam dump (green), P *vs*. XS (top), P *vs*. YS (middle), and XS *vs*. YS (bottom). In the right: lost particles from IP to upstream of collimator 1 (green), P *vs*. XS (top), P *vs*. YS (middle), and XS *vs*. YS (bottom). For extraction line with 0.75 mrad photon aperture, initial 100,000 particles are randomly distributed in *P* (0-500GeV), *XS*, and *YS*. σ_{YS} is a constant of 0.167 mrad, and σ_{XS} is varied among 0.2 mrad (red), 0.333 mrad (green), and 0.667 mrad (blue). Histograms of normalized lost-particle density (probability for particle getting lost) in *P* (top), *XS* (middle) and *YS* (bottom).

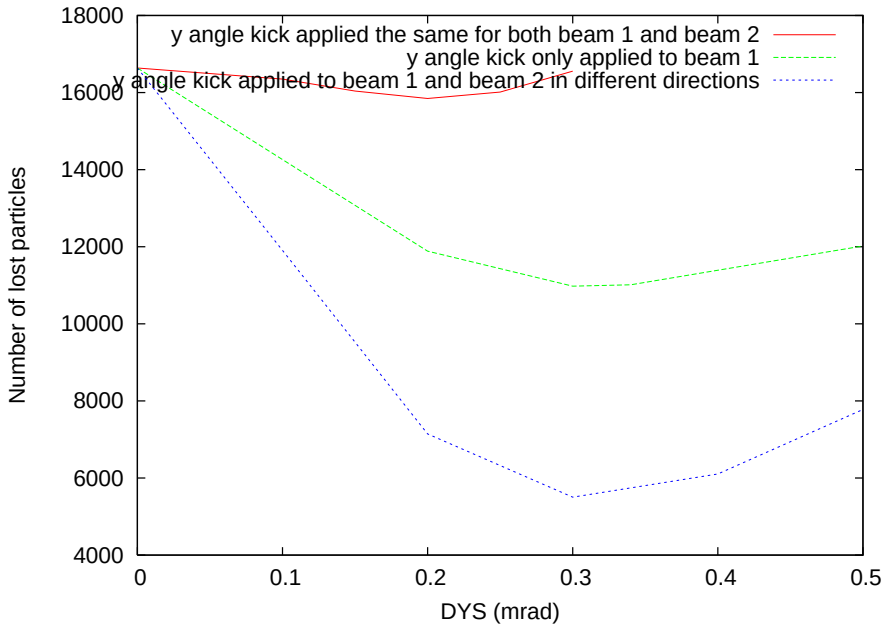

Figure 24: Number of lost particles *vs*. vertical Y-angle kick to both beam 1 and 2 right after IP (red), positive Y-angle kick only applied to beam 1 with initial negative Y-angles (green), and Y-angle kick applied to both beam 1 and 2 in different directions (positive Y-angle kick to beam 1, negative Y-angle kick to beam 2), for extraction line with 0.75 mrad photon aperture. Initial particles are: beam 1 and 2, for file $c25_dy80_hs$.